Research

Author for correspondence:
Andrei V. Komolkin
e-mail: a.komolkin@spbu.ru

Theoretically possible spatial accuracy of geomagnetic maps used by migrating animals

Andrei V. Komolkin[1], Pavel Kupriyanov[1], Andrei Chudin[1], Julia Bojarinova[1], Kirill Kavokin[1] and Nikita Chernetsov[1,2]

[1]Saint Petersburg State University, 7-9 Universitetskaya Emb., St Petersburg 199034, Russia
[2]Biological Station Rybachy, Zoological Institute RAS, Rybachy 238535, Kaliningrad Region, Russia

AVK, 0000-0002-3577-1978; PK, 0000-0002-6610-2785; AC, 0000-0003-2325-1219; JB, 0000-0003-1759-686X; KK, 0000-0002-0047-5706; NC, 0000-0001-7299-6829

Many migrating animals, belonging to different taxa, annually move across the globe and cover hundreds and thousands of kilometres. Many of them are able to show site fidelity, i.e. to return to relatively small migratory targets, from distant areas located beyond the possible range of direct sensory perception. One widely debated possibility of how they do it is the use of a magnetic map, based on the dependence of parameters of the geomagnetic field (total field intensity and inclination) on geographical coordinates. We analysed temporal fluctuations of the geomagnetic field intensity as recorded by three geomagnetic observatories located in Europe within the route of many avian migrants, to study the highest theoretically possible spatial resolution of the putative map. If migratory birds measure total field intensity perfectly and take the time of day into account, in northern Europe 81% of them may return to a strip of land of 43 km in width along one of coordinates, whereas in more southern areas such a strip may be narrower than 10 km. However, if measurements are performed with an error of 0.1%, the strip width is increased by approximately 40 km, so that in spring migrating birds are able to return to within 90 km of their intended goal. In this case, migrating birds would probably need another navigation system, e.g. an olfactory map, intermediate between the large-scale geomagnetic map and the local landscape cues, to locate their goal to within several kilometres.

1. Introduction

Many animals regularly perform long-distance movements for hundreds and thousands of kilometres, which allows them to successfully exploit seasonally available resources in the areas where survival during some part of the annual cycle is problematic or impossible [1]. Probably most widely known are migratory birds, but long-distance movements have been reported for a wide array of other taxa, e.g. fish, sea turtles [2–4], cetaceans [5] and even insects [6–8]. Many long-distance migrants show fidelity to their natal, breeding or non-breeding sites [9], which clearly demonstrates that they possess the ability to locate a rather compact goal from a large distance, beyond the possible range of direct sensory perception. This ability is usually called true navigation [10].

Two hypotheses explaining the mechanism of true long-distance navigation are currently most commonly discussed: the chemical hypothesis, which suggests that the map is based on the distribution of volatile substances in the atmosphere [11] or of soluble substances in the ocean for marine animals [12,13]; and the geomagnetic hypothesis that assumes that animals use the geomagnetic field parameters [14,15]. The physical basis of chemical map is currently less than obvious, even though research is being done in this respect [16]. Conversely, the physical parameters of the geomagnetic field, including their spatial dependence and temporal variation, are well known [17].

The geomagnetic map hypothesis assumes that migrating birds make use of the gradient map, as opposed to the mosaic map [18,19], based on the dependence of the parameters of the geomagnetic field—total intensity and inclination—on geographical coordinates. Most generally, both these parameters vary from the magnetic poles to the magnetic equator. Total intensity peaks near the poles (about 60 000 nT) and reaches a minimum (about 30 000 nT, locally down to 24 000 nT) near the equator. Inclination is the angle between the horizontal plane and the direction of the magnetic vector and it is *a priori* equal to $+90°$ at the northern magnetic pole and $-90°$ at the southern magnetic pole, and it is equal to $0°$ at the magnetic equator [17].

This is however just a very general pattern; in reality isolines of total intensity (isodynamic lines) and of inclination (isoclines) are not strictly parallel to geographical parallels and to each other. In some regions, e.g. in southern Indian Ocean, isodynamic lines and isoclines form a grid that can theoretically be used for purely magnetic navigation along the two axes (north–south and east–west), whereas in other large regions, e.g. in southern North America or in Australia, they run parallel to each other and provide no positional information along one of the axes (east–west) [20]. It means that geomagnetic map based on gradients of total field intensity and inclination can be used for bi-coordinate navigation in some regions, but not everywhere on the Earth. In many areas the second axis has to be provided by an additional cue. One theoretical possibility is to measure the angle between the magnetic north and the geographical north (magnetic declination), which is potentially an additional powerful positioning tool. At least migratory birds may theoretically use declination, because they are known to possess both celestial compass(es) for detecting the geographical north and a magnetic compass for the magnetic north [19]. However, the actual ability to detect magnetic declination and to use it in a map-related context remains to be demonstrated experimentally in any animal.

The ability of birds and sea turtles to perceive both total intensity and inclination of Earth-strength magnetic fields has been shown experimentally [21–24]. If birds [25], sea turtles [15,26,27], possibly also salmonid fishes [28,29] and other long-distance migrants use the geomagnetic field for position finding, the question inevitably arises: what is the possible accuracy of the geomagnetic map? Migratory birds are known to be able to return to their natal, former breeding or wintering sites to within several kilometres [9]. Can spatial and temporal variation of the geomagnetic field alone enable this accuracy of position finding, or does it demand using some additional mechanisms?

To return to their breeding site, migrating birds should measure total field intensity before departure and remember the value; next spring they would try to locate the site corresponding to that value by measuring the geomagnetic field total intensity. The uncertainty of site finding is contributed by three factors. Firstly, it is uncertainty of measurement of the field before departure. Secondly, it is the regular annual change of the geomagnetic field during the period between the time of imprinting of the breeding site before departure and the time of arrival in spring. Thirdly, it is uncertainty in position finding.

In this work, we analyse the limitations imposed on magnetic navigation precision by temporal fluctuations of total intensity of the geomagnetic field. We use the archived data on variation of the Earth's magnetic field during the period of 1991–2015. The data were collected in three sites in
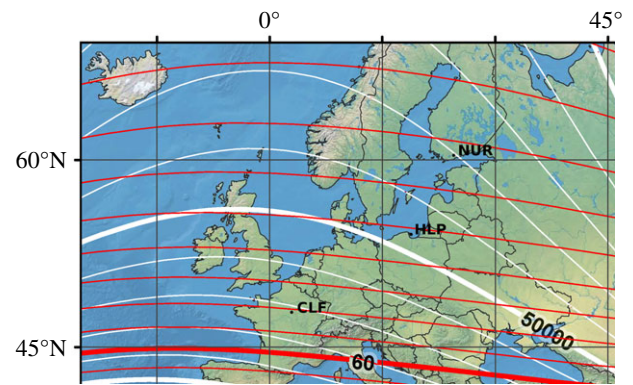
Figure 1. Map of Europe with the isolines of total magnetic field (white) and inclination (red). This map is the superposition of maps provided by WMM-2015 [31,32]. Positions of the magnetic observatories Nurmijärvi, Hel and Chambon-la-Forêt are shown.

Europe along the usual route of avian migrants. The purpose of the investigation was to find out the highest possible precision of the magnetic map which birds (or any migrating animals) can in principle achieve.

2. Material and methods

2.1. Sources of the data
The data on Earth's magnetic field variation were obtained by the INTERMAGNET [30,31] from the following magnetic observatories:

(1) NUR ($60.508°$ N, $24.655°$ E): Nurmijärvi, Finland, operated by Finnish Meteorological Institute;
(2) HLP ($54.608°$ N, $18.817°$ E): Hel, Poland, operated by Polish Academy of Sciences (data are accessible for 1998–2015);
(3) CLF ($48.017°$ N, $2.266°$ E): Chambon-la-Forêt, France, operated by Institut de Physique du Globe de Paris.

The observatories collect three components of vector of Earth's magnetic field every minute with magnetometers, which achieved a precision of 0.1 nT. Records from each of the magnetic observatories since 1991 up to now are stored on WWW-servers of INTERMAGNET and they are available for analysis. The clocks of observatories are synchronized, and time stamp of each measurement is in Coordinated Universal Time (UTC), which for the purpose of this investigation corresponds to Greenwich Mean Time (GMT). The solar (local) time in Nurmijärvi is UTC $+1$ h 40 min, in Hel it is UTC $+ 1$ h 15 min, in Chambon-la-Forêt it is UTC $+ 10$ min.

The second source of the analysed data was World Magnetic Model-2015 [32,33], which provides information on mean values of parameters of magnetic field on the surface of the Earth for the epoch 2015–2020. This source was used to analyse gradients of the total field intensity (see §2.4).

The map of magnetic field of the Earth in Europe and positions of the observatories are presented in figure 1.

2.2. Mathematical model of temporal dependence of the Earth's magnetic field
In figure 2, the total intensity of the Earth's magnetic field $B(t)$ at the location of NUR observatory during the period from the beginning of 1991 to the end of 2015 is presented: the red line shows fluctuations between daily minimal and maximal values while the blue line is the daily average values. Based on this plot, we can separate at least three components of the total intensity $B(t)$, which is recorded by the observatory

$$B(t) = B_{0,i} + b_i t + N(t). \tag{2.1}$$
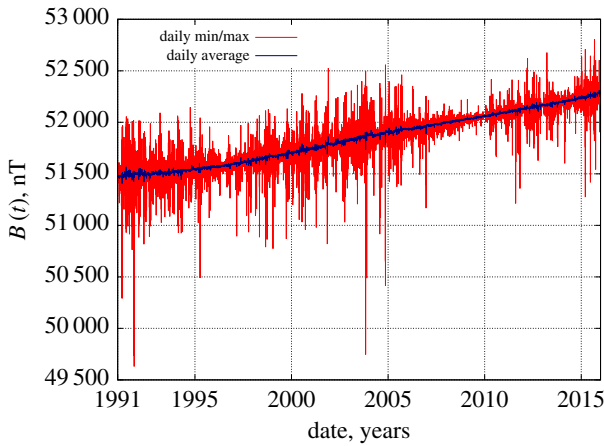
Figure 2. Total magnetic field in Nurmijärvi since the beginning of 1991 to the end of 2015. Red (grey) line shows fluctuations between minimal and maximal values registered during each day, while blue (dark grey) line is the daily average values. (Online version in colour.)

Here, $B_{0,i}$ is the intensity at the beginning of i-th year (midnight, 1 January), b_i is the linear coefficient for that year (since linear growth of the field intensity during a year is a good approximation) and $N(t)$ is the fluctuation, i.e. random variable. For instance, in 2007 it was found that $B_{0,2007} = (51\,966.3 \pm 0.4)$ nT and $b_{2007} = (0.98 \pm 0.02)\,10^{-6}$ nT s^{-1}, which is equal to (30.8 ± 0.8) nT yr^{-1}.

To analyse fluctuations, the linear growth of the intensity was subtracted from the recorded values of $B(t)$

$$N(t) = B(t) - B_{0,i} - b_i t, \qquad (2.2)$$

so the average of $N(t)$ is equal to zero during each year and, totally, during the observation period 1991–2015.

2.3. Methods of statistical analysis

Autocorrelation function $C(\Delta t)$ of the fluctuations $N(t)$ was calculated for the whole period of 25 years

$$C(\Delta t) = \int_{1991}^{2015} N(t)N(t + \Delta t)\,\mathrm{d}t, \qquad (2.3)$$

where Δt was chosen from 0 to 5 days with step of 1 min. The plot of $C(\Delta t)$ is shown in figure 3a. Obviously, there are two types of correlations, which correspond to two modes of magnetic field fluctuations. The correlations of first type are caused by daily rotation of the Earth. They are regular and, possibly, oscillating. Their autocorrelation function consists of two cosine functions with periods of one day and half a day. Since the position of Sun with respect to the zenith and nadir influences these regular fluctuations, they are linked to the phase of the rotation of the Earth, i.e. to the local solar time at the site of the magnetic observatory. The physical reason of these regular changes is the solar wind, which interacts with the magnetic field and atmosphere of the Earth differently on the dayside and nightside hemispheres [34]. This part of autocorrelation function is seen very clearly for $\Delta t > 3$ days, and it continues for a long time, months and longer (not shown in figure 3a). The correlations of second type are random. This part of autocorrelation function has the form of exponential decay with oscillations.

In this work, the autocorrelation function was approximated by four functions (figure 3b)

$$\begin{aligned} C(\Delta t) &\approx f_1(\Delta t) + f_2(\Delta t) + f_3(\Delta t) + f_4(\Delta t) \\ &= a_1\cos(2\pi\Delta t) + a_2\cos(4\pi\Delta t) \\ &\quad + a_3\exp\left(\frac{-\Delta t}{T_3}\right)\cos(2\pi\Delta t) + a_4\exp\left(\frac{-\Delta t}{T_4}\right)\cos(4\pi\Delta t). \end{aligned} \qquad (2.4)$$

Here, time Δt is measured in days. Decay time T_3 is equal to 0.75 day (18 h) and T_4 is equal to 0.08 day (about 2 h). Such fluctuations are slow when compared with the period of time during which migratory birds should measure and, possibly, over which they should average the values of total field. Dispersions of these fluctuations ($a_3 = 270$ nT^2 and $a_4 = 305$ nT^2) are approximately the same, exceeding the dispersion of regular oscillations of the magnetic field $a_1 = 98$ nT^2 and $a_2 = 38$ nT^2. Fast correlations with the decay time of a few minutes are weak, their dispersion is negligible.

As $N(t)$ is a random variable with observed values $r_i = N(t_i)$, which are stored in the analysed files, it was possible to estimate its probability density $p(N)$. A priori we should not assume normal (Gaussian) distribution of the noise. Moreover, probability density functions may be different at different times of year: close to June and December solstices, around spring and autumn equinoxes. We analysed fluctuations separately for three periods: the period of spring migration April–May, summer (imprinting) time July–August, and the autumn migratory period September–October. Lengths of the periods were 61–62 days; the number of years was 25. Taking into account regular oscillations during a day, it is useful to calculate probability density $p_h(N)$ for different time h of the day. In this work, 24 different functions $p_h(N)$ were calculated for each hour during the day (using UTC, but not the local time): $p_0(N)$ was calculated for data between 00.00 and 00.59 UTC, $p_1(N)$ was calculated for data between 01.00 and 01.59 UTC, and so long. Figure 4 summarizes how to select proper time periods to calculate probability density functions. Example of the probability density functions are shown in figure 5a.

Probability P to find realization of the random variable N in the range from N_1 to N_2 around the most probable value N_0 is calculated as

$$P = \int_{N_1}^{N_2} p_h(N)\,\mathrm{d}N. \qquad (2.5)$$

If the values are chosen as $N_1 < N_0 < N_2$ and $p_h(N_1) = p_h(N_2)$ then $P\cdot100\%$ of all measurements fall inside the range $[N_1 \ldots N_2]$ around the most probable value. Illustration of how to find these ranges for $P = 50\%$ and $P = 90\%$ is shown in figure 5b.

2.4. Spatial distribution of the magnetic field, its gradient

The World Magnetic Model-2015 [32,33] provides data on mean (expected) values of certain parameters of the geomagnetic field in past and future (until 2020 with a step of 1 day) all around the world. These data do not include random variation but rather include regular yearly changes of the parameters of the field.

In this work, the distribution of the total magnetic field was analysed to calculate its gradient. The values of the intensity were obtained on 1 January 2015, at the site of each observatory and in the positions $\pm 1°$ along circle of latitude (parallel) and meridian from the site. The differences of the values along parallel and meridian allow us to estimate gradient in the units of nT/° and recalculate them in Cartesian coordinates in the units of nT km^{-1} taking into account length of the arc of 1° along parallel and meridian. Along meridian this length is 111.1 km, but along the circle of latitude it is $111.3 \times \cos(\theta)$ km, where θ is the latitude. For instance, in Nurmijärvi it is 54.8 km, in Hel it is 64.5 km, in Chambon-la-Forêt it is 74.4 km.

In Nurmijärvi, the components of the gradient are 237.4 nT/° along the meridian (2.14 nT km^{-1}, directed to the north) and 72.3 nT/° along the parallel (1.30 nT km^{-1}, directed to the east). The gradient of the total magnetic field is 2.50 nT km^{-1} and directed at an angle 31.3° from the meridian to the northeast (NE).

This gradient means that if two magnetometers, which are placed in different positions, detect *at the same time* two values of
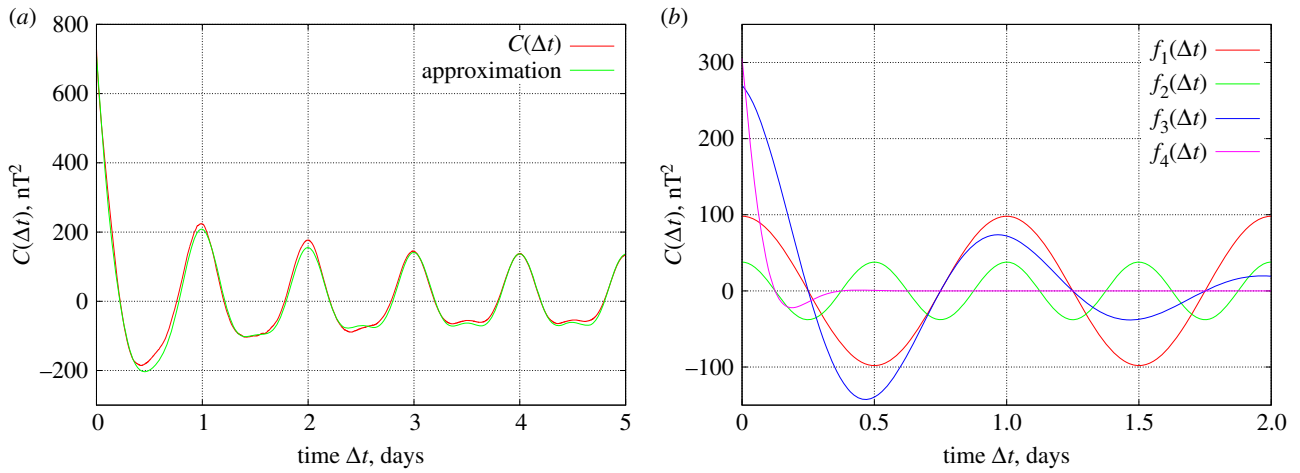
Figure 3. Autocorrelation function of random variable $N(t)$: (*a*) function and its approximation, (*b*) four components of approximation according to formula (2.3). (Online version in colour.)
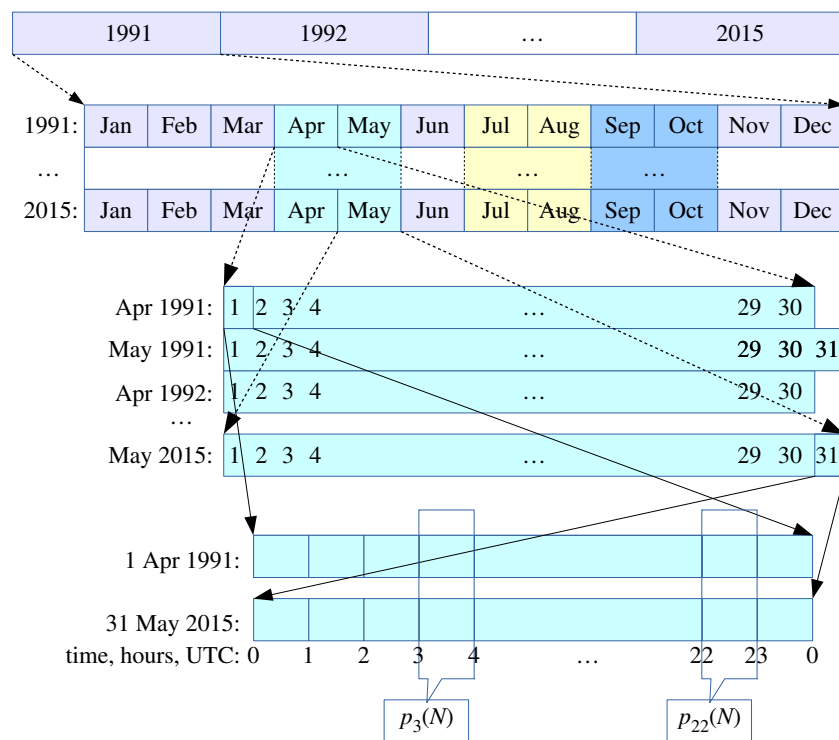
Figure 4. Algorithm of data extracting, used to calculate probability density functions $p_h(N)$. Consequence steps are shown for the spring migratory period April – May as an example. The $p_3(N)$, for instance, is based on the records of the total magnetic field each minute between 03.00 and 03.59 UTC each day of each April and May since 1991 to 2015.

the total magnetic field that differ by 2.5 nT, then their positions on the ground differ by 1 km in direction perpendicular to isodynamic line. But for one unmovable magnetometer (with fixed position) this means that if it measures two values *at different times* and the values differ by 2.5 nT, then the current instant coordinate of the isodynamic line shifts by 1 km on the ground relative to the position of the isoline at the time of previous measurement.

3. Results

3.1. Total field intensity in Nurmijärvi

In Nurmijärvi, total intensity of the geomagnetic field between 1991 and late 2015 grew on average by 32.5 nT per year (figure 2). The gradient of the total magnetic field is 2.50 nT km^{-1} and directed at an angle 31.3° from the meridian

to the NE. Growth of the intensity leads to shifting the isodynamic line by 13 km per annum towards the southwest.

Autocorrelation function of $N(t)$ shows (figure 3) that the fluctuations of the random variable are dependent on the time of the day, i.e. on the position of the Sun relative to the Earth. The probability density of magnetic field fluctuations $p_{14}(N)$ for the period of 14.00–14.59 and $p_{23}(N)$ for 23.00–23.59 UTC in Nurmijärvi, which approximately correspond to 15.40–16.39 and 0.40–1.39 of the local time, are shown in figure 5*a*. The distributions are not symmetric with respect to their maxima, i.e. the random variable does not have the normal (Gaussian) distribution. The most probable values N_0 (maximum of the probability density function) of these two functions coincide, but the strongest fluctuations have positive values in the daytime and negative values at night.
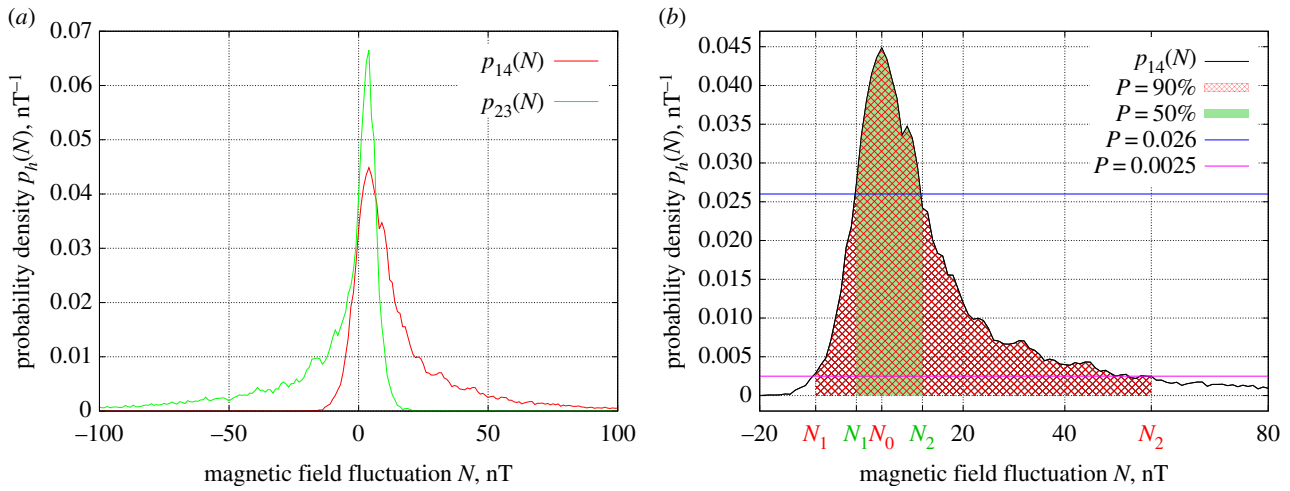
Figure 5. Probability density functions: (a) two functions in day time (14.00–14.59, $p_{14}(N)$, red line) and at night (23.00–23.59, $p_{23}(N)$, green) in Nurmijärvi; (b) explanation on the choosing of the parameters N_1 and N_2 in the formula (2.5): the areas, filled under the curve, are 50% (solid green) and 90% (crossed red) of the total area under the curve $p_{14}(N)$. Colours of interval boundaries N_1 and N_2 correspond to the colours of the areas. N_0 is the maximum probability in this period.
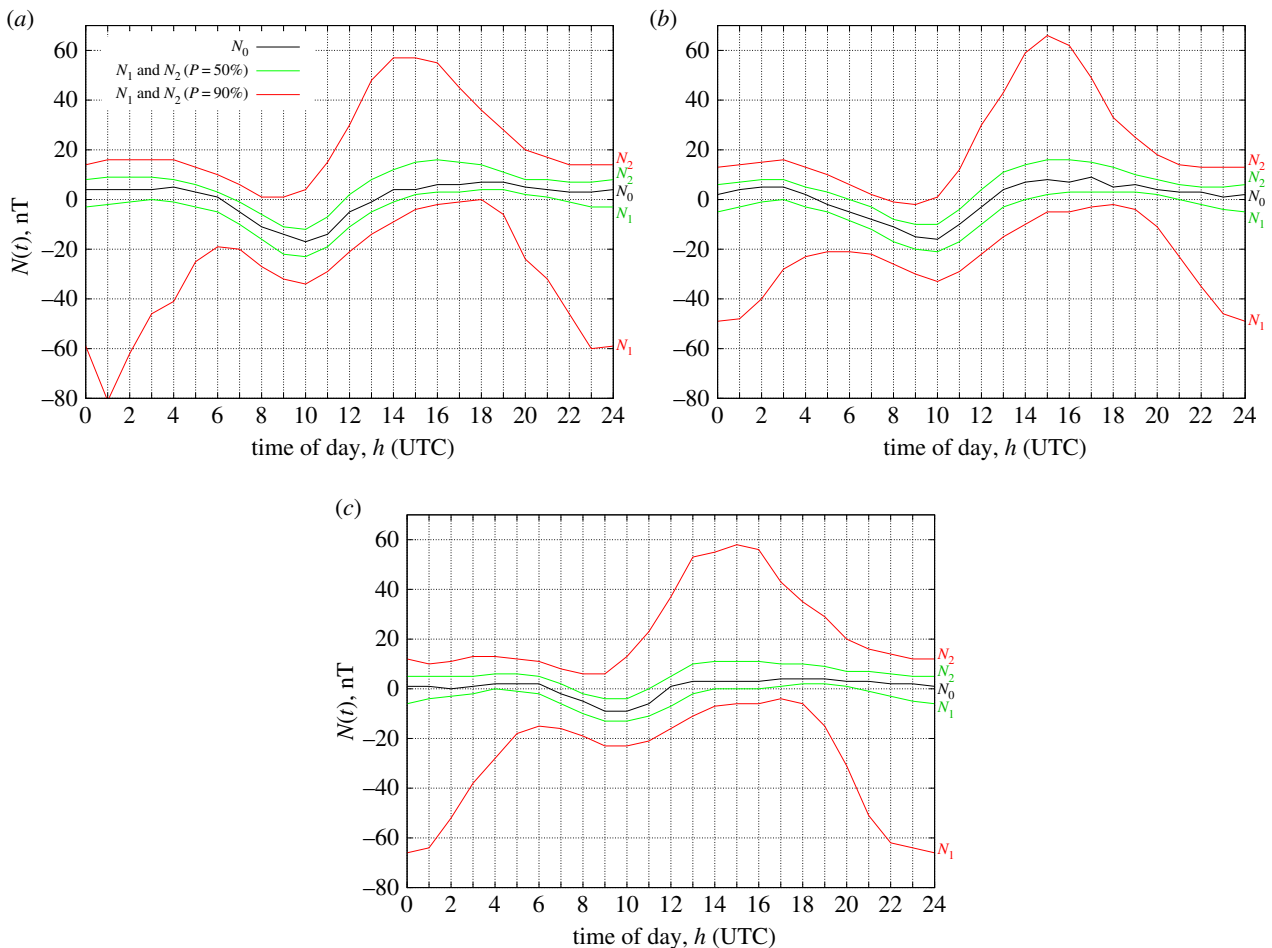
Figure 6. Daily behaviour of N_0, bounds N_1 and N_2 of ranges for $P = 50\%$ and 90% are shown for the spring (a), summer (b) and autumn (c) periods in Nurmijärvi (NUR). Colours of the lines correspond to the colours in figure 5b. (Online version in colour.)

In figure 6, the plots of daily behaviour of the most probable value N_0, bounds of ranges (N_1 and N_2) for $P = 50\%$ and 90% are shown for the spring (figure 6a), summer (figure 6b) and autumn (figure 6c) periods in Nurmijärvi. The graphs show that during a major part of the day (from 14.00 to 05.00 UTC including nighttime) the value N_0 changes weakly, but from 06.00 to 13.00 UTC the value decreases and reaches its minimum at 09.00–10.00 UTC, which is close to noon of the local time. Fifty per cent of measurements fall into a zone with the width $N_2 - N_1 \approx 12$ nT. This zone symbatically varies with N_0. The area into which 90% of measurements fall is asymmetric: at night (from 19.00 to 05.00 UTC) the lower bound of this area drops to lower magnetic fields, while in the afternoon (11.00–16.00 UTC) the upper bound rises. For instance, in the spring period at approximately 01.00 UTC, 50% of measurements fall into the range from $N_1 = -2$ nT to $N_2 = +9$ nT
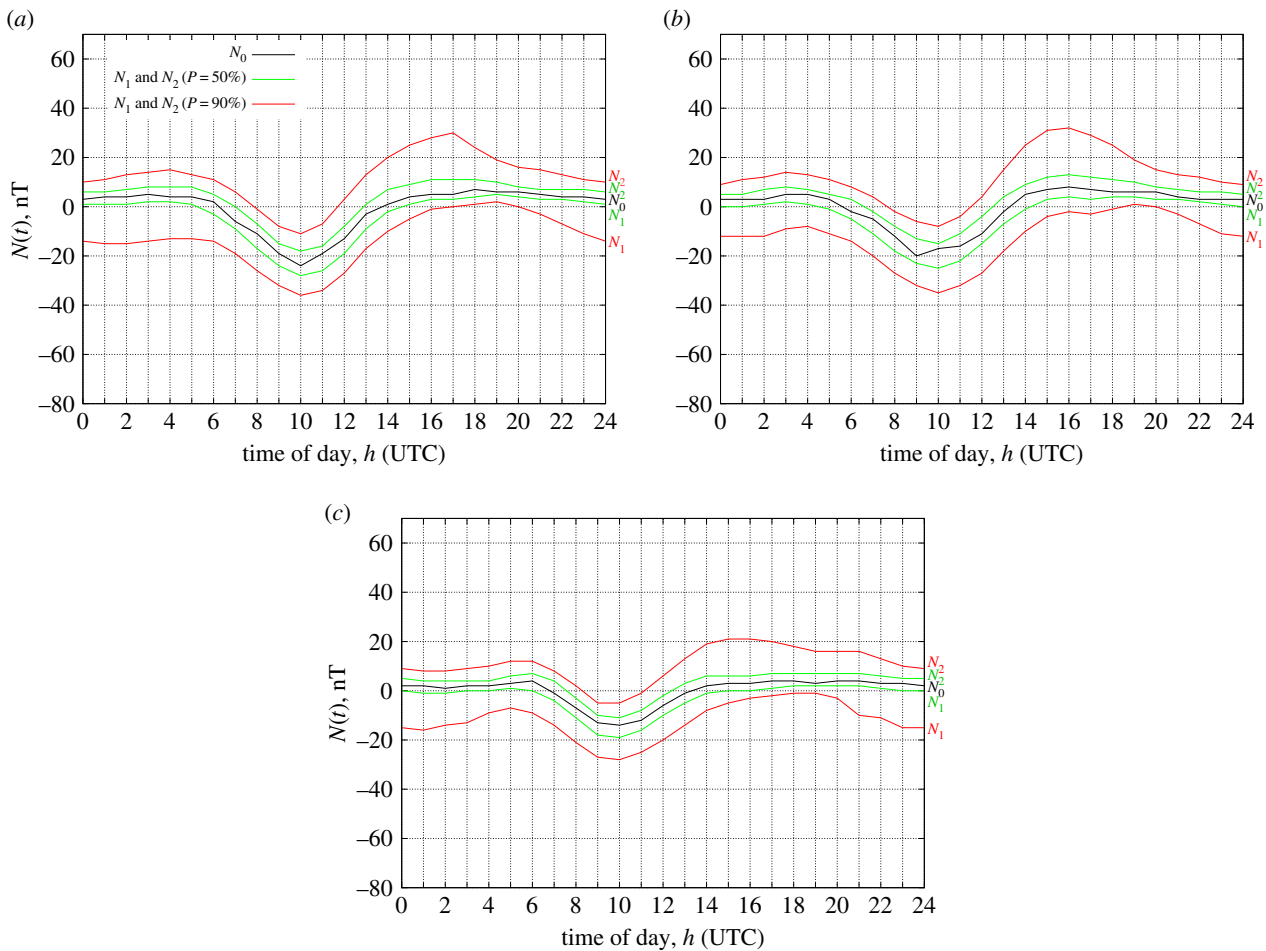
Figure 7. Daily behaviour of N_0, bounds N_1 and N_2 for $P = 50\%$ and 90% ranges are shown for the spring (a), summer (b) and autumn (c) periods in Hel (HLP). Colours of the lines correspond to the colours in figure 5b. (Online version in colour.)

(width of the range is equal to 11 nT), but 90% of measurements are in the range from $N_1 = -80$ nT to $N_2 = +16$ nT (width of the range is equal to 96 nT). On the contrary, the measurements performed in day time (14.00 UTC) fall into ranges $[-1 \ldots +11]$ nT ($P = 50\%$) and $[-9 \ldots +57]$ nT ($P = 90\%$), respectively.

3.2. Total field intensity in Hel

At Hel station in northern Poland the total magnetic field increased during 1998–2015 by 609 nT with a rate of 33.8 nT yr^{-1}. Gradient of the total magnetic field is equal to 2.30 nT km^{-1} and directed at an angle of 29.1° from the meridian to the NE. The plots of daily behaviour of N_0, N_1 and N_2 for $P = 50\%$ and 90% are shown in figure 7. The most precise evaluation of the mean intensity can be obtained from measurements performed at 19.00–21.00 UTC (90% of measurements fall within a 17 nT range corresponding to a 7.5 km wide strip). The worst precision (30 nT or 13 km) is realized at 12.00–17.00 UTC. The southwest (SW) yearly shift of the isodynamic line amounts to 14.7 km.

3.3. Total field intensity in Chambon-la-Forêt

At Chambon-la-Forêt observatory in France, the total field increased with a mean rate of 26.7 nT yr^{-1} during the last 25 years. Gradient of the total magnetic field is equal to 2.76 nT km^{-1} and directed at an angle of 11.8° from the meridian to the northnortheast. The shift of the isodynamic line near CLF is about 9.6 km per year towards southsoutheast.

The most probable field value N_0 and range boundaries N_1 and N_2 of 50% and 90% field variation as functions of

time of the day in the three periods are plotted in figure 8. In spring, 50% of field measurements would be scattered within the range of 4–6 nT at night and up to 10 nT near noon, which would correspond to a strip of land not more than 3.5 km in width. In total, 90% of measurements would have variation from 13 nT at night to 26 nT in the daytime, corresponding to 5 and 10 km on land, respectively.

We note that in this region fluctuations of the geomagnetic field are much weaker than in northern Europe. A comparison of fluctuation densities at nighttime in spring in CLF, HLP and NUR is presented in figure 9. One can see that fluctuations towards stronger fields are similar for all the observation sites, but the further south the site is, the smaller the fluctuations towards weaker fields are.

4. Discussion

### 4.1. Assumption on bird magnetic sensor precision

There exists only limited information about the possible precision of determination of magnetic intensity among different animals. For example, neurophysiological responses by birds to changes in intensity as small as 0.05–0.2 µT were reported [35,36].

In this work, two alternative assumptions were made about the precision of magnetic sensing of birds:

(1) Birds are able to measure the parameters of Earth's magnetic field with absolute precision, i.e. with insignificant error, like quantum magnetometers used in the
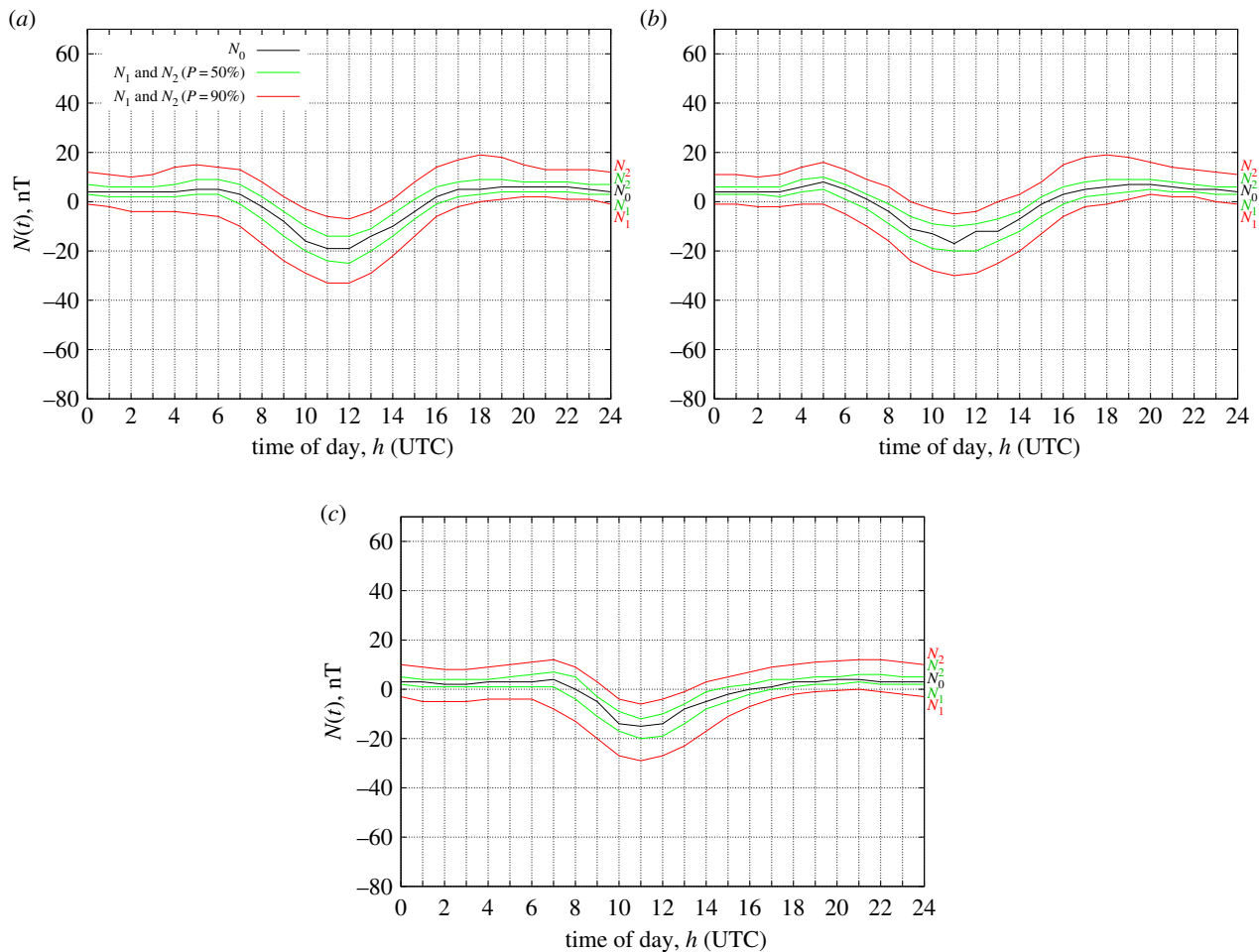
Figure 8. Daily behaviour of N_0, bounds N_1 and N_2 of ranges for $P = 50\%$ and 90% are shown for the spring (*a*), summer (*b*) and autumn (*c*) periods in Chambon-la-Forêt (CLF). Colours of the lines correspond to the colours in figure 5*b*. (Online version in colour.)
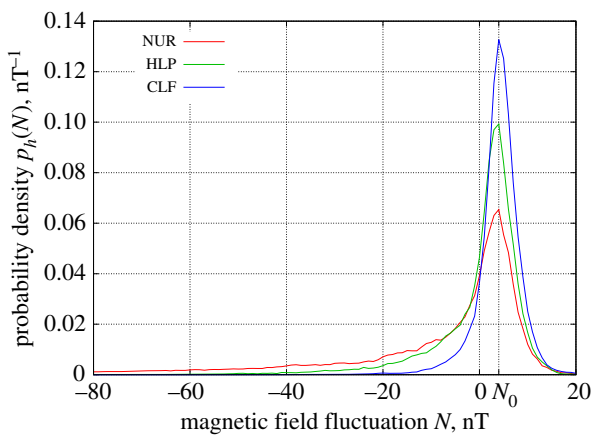
Figure 9. Probability densities $p(N)$ of night fluctuations in the three sites. Here, the probability densities $p(N)$ are calculated for the 3 h time interval 23.00–01.59 UTC, i.e. $p(N) = (p_{23}(N) + p_0(N) + p_1(N))/3$. (Online version in colour.)

observatories [37]. This is an idealized case, which leads to minimal uncertainty of position finding.

(2) Birds are able to make measurements of total field intensity with a relative accuracy of 0.1% (i.e. about 50 nT), as suggested in [35,36].

4.2. Finding the position on the migration route

Let us consider navigation of a bird which has in its memory a map based on the geomagnetic field intensity (for instance,

learned from previous journeys). This would mean that certain values of the field intensity would be interpreted by the bird as signals to take certain actions (e.g. changing flight direction, stopping over for refuelling or looking out for places for breeding or wintering). As follows from the analysis above, the uncertainty of *geographical* position finding from such a magnetic map would be different for different parts of the European route.

If the magnetic sensor of migratory birds measures total intensity with absolute precision, then in northeastern Europe (Finland, northwest Russia) 50% of birds would determine their position within a strip of 5 km in width with respect to *the average position of isodynamic line*, and 90% of birds in a strip of 25–35 km in width, determined by fluctuation of the Earth's magnetic field. But the isodynamic line is not immobile during a day: its most probable position in the day time shifts to NE as far as 10 km with respect to the position at night. This is an additional source of uncertainty of the magnetic map. Variation of these parameters during a day is shown in figure 6. If the precision of the bird's magnetometer is 50 nT, then the widths of the corresponding strips are 44 km and 65–80 km.

In the eastern Baltic region, the uncertainty would be less: with 90% confidence the coordinate along the maximum gradient (SW–NE) direction can be determined to 7.5 km. If the measurement precision is limited to 0.1% (50 nT), the width of the error strip increases by 43 km. The yearly shift of the isodynamic line is 13 km.

In southwestern Europe (central France), the uncertainty of position finding due to fluctuations is even smaller: 5 km with 90% confidence. With the measurement precision of

0.1% (50 nT), the error strip increases by 36 km. The yearly shift of the isodynamic line is 9.6 km to southsoutheast.

Thus, the magnetic map is able to provide the precision of position finding on the European bird migration route within several tens of kilometres, which seems sufficient for long-range navigation. In Central and South Europe, provided absolute precision of field measurement and optimized timing of magnetic reckoning, it gives geographical position with the accuracy of several kilometres, which is arguably enough for further refining the position (e.g. for homing or finding breeding sites) using visual cues.

The regular shift of isodynamic lines (by 10–15 km per year in the modern epoch) means that a magnetic map older than 10 years would accumulate an error of over 100 km, which would render it nearly useless. It might be the main reason for learning the map by every generation of migrants anew and the lack of inherited maps, which is the view shared by most researchers of avian migration [19,38].

The largest uncertainty of position finding due to short-time fluctuations occurs in NE Europe, where many regular migrants have their breeding grounds. In the next subsection, we consider the problem of return to the breeding site in NE Europe using magnetic navigation.

4.3. Site fidelity in northeast Europe

Experiments of the translocation of nestlings and fledglings of several migratory bird species from the birthplace to other remote regions demonstrated that yearlings return not to their birthplace but to sites they memorize during the imprinting period within their first summer (for review see [9]). For example, pied flycatchers (*Ficedula hypoleuca*), long-distance migrants wintering in Central Africa and showing a high level of site fidelity (philopatry), imprint their future breeding place at the age of 35–50 days [9]. The estimated period of imprinting in this species for the latitude of Nurmijärvi is the second part of August (calculated on the basis of median egg laying date for southwestern Finland [39] and southern Karelia [40]). Spring migration of pied flycatchers in these regions is recorded mainly in the second ten days of May, but first birds may be seen from the very end of April [39,40]. The possible periods of imprinting (15–30 August) and spring arrival (6–20 May) of pied flycatchers are included in the periods we analysed in this paper (July–August and April–May).

Consider the case of the most precise positioning of the birds returning to Nurmijärvi. The fluctuations of the magnetic field are minimal at 07.00 UTC both in spring and summer. The time interval between the period of imprinting in summer and arrival to breeding ground in spring is about 10 months. During this time, due to the yearly trend of field intensity the field increases by 27 nT, which corresponds to isodynamic line shift of 11 km to SW. This shift of isoline together with fluctuations lead to the distribution of returning migrants with centre at *minus* 10 km of the departure place (i.e. 10 km SW); 25% of birds would get into the area between −11.5 and −8.5 km, and 81% in the strip from −16 km to −4 km of their departure point. This means that most of the returning migrants would stay several kilometres SW of the departure site.

If migrating birds measure total field intensity at sunrise or sunset, the uncertainty increases with respect to the absolute minimum which occurs at 07.00 UTC. The birds are known to have an internal clock [41,42], so measuring the

Table 1. Approximate time of sunrise and sunset in Nurmijärvi.

date (spring)	date (autumn)	sunrise time (UTC)	sunset time (UTC)
1 April	10 September	03.40	17.00
1 May	12 August	02.20	18.30
31 May	12 July	01.10	19.40

magnetic field at a certain time of day (e.g. at sunrise or sunset) is a realistic assumption.

During the periods of imprinting and spring arrival, sunrise and sunset in Nurmijärvi are close in time, night is very short. At sunset (table 1) the second deepest minimum of magnetic fluctuations is observed, while at sunrise the geomagnetic field is most unstable (figure 6). If a pied flycatcher measures the magnetic field with absolute accuracy at sunset, then 25% of birds would return in the strip of $[-12\ldots -8]$ km, and 81% in the strip of $[-23\ldots +3]$ km with respect to the departure place.

If the measurements of field intensity are performed not with perfect accuracy, but rather with an error not exceeding 0.1% [35,36], uncertainty of position finding additionally increases. As a result, in spring 25% of birds would be able to return only within $[-34\ldots +12]$ km of the place they imprinted the previous season. Thus migrating birds would need some other navigation system, intermediate between the large-scale geomagnetic map and the local landscape cues, to locate their goal to within several kilometres. One possibility is that they may use an olfactory map for this purpose [11,43].

5. Conclusion

We analysed regular and random variations of the geomagnetic field total intensity for three geomagnetic stations situated in northeast Europe (Nurmijärvi), east Baltic region (Hel) and central France (Chambon-la-Forêt) and used the results to estimate the applicability of this geophysical parameter as a basis for a magnetic map for birds migrating across the European continent. Total intensity gives one of two necessary coordinates for navigation. Our results show in principle the possibility of long-range magnetic navigation if the geomagnetic field is measured with a precision better than 0.1% at the optimal time of the day. Regular many-year trend of isodynamic geomagnetic lines creates insuperable problems for using inherited magnetic maps by inexperienced first-year migrants. So, every generation of migrants should learn magnetic map anew. Large random variations of the geomagnetic intensity in NE Europe limit the precision of finding the breeding site by migratory birds nesting in that region (as, for example, pied flycatchers) to several tens of kilometres, which suggests the necessity of another navigation mechanism to provide the observed breeding site fidelity of such species.

References

1. Alerstam T. 2006 Conflicting evidence about long-distance animal navigation. *Science* **313**, 791–794. (doi:10.1126/science.1129048)

2. Quinn TP. 1991 Models of Pacific salmon orientation and navigation on the open ocean. *J. Theor. Biol.* **150**, 539–545. (doi:10.1016/S0022-5193(05)80445-X)

3. Lohmann KJ, Lohmann CMF, Endres CS. 2008 The sensory ecology of ocean navigation. *J. Exp. Biol.* **211**, 1719–1728. (doi:10.1242/jeb.015792)

4. Gould JL, Gould CG. 2012 *Nature's compass: the mystery of animal navigation.* Princeton, NJ: Princeton University Press.

5. Walker MM, Kirschvink JL, Ahmed G, Dizon AE. 1992 Evidence that fin whales respond to the geomagnetic field during migration. *J. Exp. Biol.* **171**, 67–78.

6. Holland RA, Wikelski M, Wilcove DS. 2006 How and why do insects migrate? *Science* **313**, 794–796. (doi:10.1126/science.1127272)

7. Chapman JW, Reynolds DR, Wilson K. 2015 Long-range seasonal migration in insects: mechanisms, evolutionary drivers and ecological consequences. *Ecol. Lett.* **18**, 287–302. (doi:10.1111/ele.12407)

8. Warrant E, Frost B, Green K, Mouritsen H, Dreyer D, Adden A, Brauburger K, Heinze S. 2016 The Australian Bogong moth *Agrotis infusa*: a long-distance nocturnal navigator. *Front. Behav. Neurosci.* **10**, 77. (doi:10.3389/fnbeh.2016.00077)

9. Sokolov L. 1997 Philopatry of migratory birds. In *Physiology and general biology reviews*, vol. 11 (ed. TM Turpaev), pp. 1–58. Amsterdam, The Netherlands: Harwood Academic Press.

10. Griffin DR. 1952 Bird navigation. *Biol. Rev. Camb. Phil. Soc.* **27**, 359–400. (doi:10.1111/j.1469-185X.1952.tb01509.x)

11. Gagliardo A. 2013 Forty years of olfactory navigation in birds. *J. Exp. Biol.* **216**, 2165–2171. (doi:10.1242/jeb.070250)

12. Lohmann KJ, Hester JT, Lohmann CMF. 1999 Long-distance navigation in sea turtles. *Ethol. Ecol. Evol.* **11**, 1–23. (doi:10.1080/08927014.1999.9522838)

13. Endres CS, Putman NF, Ernst D, Kurth J, Lohmann CM, Lohmann KJ. 2016 Multi-modal homing in sea turtles: modeling dual use of geomagnetic and chemical cues in island-finding. *Front. Behav. Neurosci.* **10**, 19. (doi:10.3389/fnbeh.2016.00019)

14. Gould JL. 1982 The map sense of pigeons. *Nature* **296**, 205–211. (doi:10.1038/296205a0)

15. Putman NF, Endres CS, Lohmann CMF, Lohmann KJ. 2011 Longitude perception and bicoordinate magnetic maps in sea turtles. *Curr. Biol.* **21**, 463–466. (doi:10.1016/j.cub.2011.01.057)

16. Wallraff HG. 2013 Ratios among atmospheric trace gases together with winds imply exploitable information for bird navigation: a model elucidating experimental results. *Biogeosciences* **10**, 6929–6943. (doi:10.5194/bg-10-6929-2013)

17. Skiles DD. 1985 The geomagnetic field: its nature, history and biological relevance. In *Magnetite biomineralization and magnetoreception in organisms: a new biomagnetism* (eds JL Kirschvink, DS Jones, BJ MacFadden), pp. 43–102. New York, NY: Plenum Press.

18. Wallraff HG. 1974 *Das Navigationssystem der Vögel*. München, Germany: R. Oldenbourg.

19. Wiltschko R, Wiltschko W. 2015 Avian navigation: a combination of innate and learned mechanisms. *Adv. Study Behav.* **47**, 229–310. (doi:10.1016/bs.asb.2014.12.002)

20. Boström JE, Åkesson S, Alerstam T. 2012 Where on earth can animals use a geomagnetic bi-coordinate map for navigation? *Ecography* **35**, 1039–1047. (doi:10.1111/j.1600-0587.2012.07507.x)

21. Mora CV, Davison M, Wild JM, Walker MM. 2004 Magnetoreception and its trigeminal mediation in the homing pigeon. *Nature* **432**, 508–511. (doi:10.1038/nature03077)

22. Mora CV, Acerbi ML, Bingman VP. 2014 Conditioned discrimination of magnetic inclination in a spatial-orientation arena task by homing pigeons (*Columba livia*). *J. Exp. Biol.* **217**, 4123–4131. (doi:10.1242/jeb.101113)

23. Lohmann KJ, Lohmann CMF. 1994 Detection of magnetic inclination angle by sea turtles: a possible mechanism for determining latitude. *J. Exp. Biol.* **194**, 23–32.

24. Lohmann KJ, Lohmann CMF. 1996 Detection of magnetic field intensity by sea turtles. *Nature* **380**, 59–61. (doi:10.1038/380059a0)

25. Kishkinev D. 2015 Sensory mechanisms of long-distance navigation in birds: a recent advance in the context of previous studies. *J. Ornithol.* **156**, 145–161. (doi:10.1007/s10336-015-1215-4)

26. Putman NF, Verley P, Endres CS, Lohmann KJ. 2015 Magnetic navigation behavior and the oceanic ecology of young loggerhead sea turtles. *J. Exp. Biol.* **218**, 1044–1050. (doi:10.1242/jeb.109975)

27. Lohmann KJ, Putman NF, Lohmann CMF. 2012 The magnetic map of hatchling loggerhead sea turtles. *Curr. Opin. Neurobiol.* **22**, 336–342. (doi:10.1016/j.conb.2011.11.005)

28. Putman NF, Lohmann KJ, Putman EM, Quinn TP, Klimley AP, Noakes DLG. 2013 Evidence for geomagnetic imprinting as a homing mechanism in Pacific salmon. *Curr. Biol.* **23**, 312–316. (doi:10.1016/j.cub.2012.12.041)

29. Putman NF, Scanlan MM, Billman EJ, O'Neil JP, Couture RB, Quinn TP, Lohmann KJ, Noakes DLG. 2014 An inherited magnetic map guides ocean navigation in juvenile Pacific salmon. *Curr. Biol.* **24**, 446–450. (doi:10.1016/j.cub.2014.01.017)

30. Love JJ, Chulliat A. 2013 An international network of magnetic observatories. *Eos* **94**, 373–384. (doi:10.1002/2013EO420001)

31. INTERMAGNET. 2015 http://www.intermagnet.org/

32. Chulliat A *et al.* 2014 *The US/UK World Magnetic Model for 2015–2020*. Boulder, CO: NOAA National Geophysical Data Center.

33. WMM. 2015 See http://www.ngdc.noaa.gov/geomag/WMM/DoDWMM.shtml.

34. Fu HS, Tu J, Song P, Cao JB, Reinisch BW, Yang B. 2010 The nightside-to-dayside evolution of the inner magnetosphere: imager for Magnetopause-to-Aurora Global Exploration Radio Plasma Imager observations. *J. Geophys. Res. Space Phys.* **115**, A04213. (doi:10.1029/2009JA014668)

35. Beason RC, Semm P. 1987 Magnetic responses of the trigeminal nerve system of the bobolink (*Dolichonyx oryzivorus*). *Neurosci. Lett.* **80**, 229–234. (doi:10.1016/0304-3940(87)90659-8)

36. Semm P, Beason RC. 1990 Responses to small magnetic variations by the trigeminal system of the bobolink. *Brain Res. Bull.* **25**, 735–740. (doi:10.1016/0361-9230(90)90051-Z)

37. Chizhik VI, Chernyshev YS, Donets AV, Frolov VV, Komolkin AV, Shelyapina MG. 2014 *Magnetic resonance and its applications*. London, UK: Springer.

38. Berthold P. 1996 *Control of bird migration*. London, UK: Chapman and Hall.

39. Ahola M, Laaksonen T, Sippola K, Eeva T, Rainio K, Lehikoinen E. 2004 Variation in climate warming along the migration route uncouples arrival and breeding dates. *Glob. Change Biol.* **10**, 1610–1617. (doi:10.1111/j.1365-2486.2004.00823.x)

40. Artemyev AV. 2008 *Population ecology of the pied flycatcher in the northern part of the range*. Moscow, Russia: Nauka.

41. Gwinner E. 1986 *Circannual rhythms*. Heidelberg, Germany: Springer.

42. Wikelski M, Martin LB, Scheuerlein A, Robinson MT, Robinson ND, Helm B, Hau M, Gwinner E. 2008 Avian circannual clocks: adaptive significance and possible involvement of energy turnover in their proximate control. *Phil. Trans. R. Soc. B* **363**, 411–423. (doi:10.1098/rstb.2007.2147)

43. Wallraff HG. 2005 *Avian navigation: pigeon homing as a paradigm*. Heidelberg, Germany: Springer.